Biogeosciences Discuss., 12, 12121–12156, 2015
www.biogeosciences-discuss.net/12/12121/2015/
doi:10.5194/bgd-12-12121-2015


Biogeosciences Discussions
Open Access



# Phototrophic pigment diversity and picophytoplankton abundance in permafrost thaw lakes

**A. Przytulska[1,2], J. Comte[1,2,3], S. Crevecoeur[1,2,3], C. Lovejoy[1,2,3], I. Laurion[4], and W. F. Vincent[1,2]**

[1]Centre d'études nordiques (CEN) and Département de biologie, Université Laval, Québec City, QC G1V 0A6, Canada
[2]Takuvik Joint International Laboratory, Centre National de la Recherche Scientifique (France, CNRS UMI 3376) and Département de Biologie, Université Laval, Québec City, QC G1V 0A6, Canada
[3]Institut de Biologie Intégrative et des Systèmes (IBIS), Université Laval, Québec City, QC G1V 0A6, Canada
[4]Centre d'études nordiques (CEN) and Centre Eau Terre Environnement, Institut national de la recherche scientifique (INRS-ETE), Québec City, QC G1K 9A9, Canada

Received: 26 June 2015 – Accepted: 13 July 2015 – Published: 4 August 2015

Correspondence to: A. Przytulska (anna.przytulska@ulaval.ca)

Published by Copernicus Publications on behalf of the European Geosciences Union.







## Abstract

Permafrost thaw lakes (thermokarst lakes) are widely distributed across the northern landscape, and are known to be biogeochemically active sites that emit large amounts of carbon to the atmosphere as $CH_4$ and $CO_2$. However, the abundance and composition of the photosynthetic communities that consume $CO_2$ have been little explored in this ecosystem type. In order to identify the major groups of phototrophic organisms and their controlling variables, we sampled 12 permafrost thaw lakes along a permafrost degradation gradient in northern Québec, Canada. Additional samples were taken from 5 rock-basin reference lakes in the region to determine if the thaw waters differed in limnological properties and phototrophs. Phytoplankton community structure was determined by high performance liquid chromatography analysis of their photoprotective and photosynthetic pigments, and autotrophic picoplankton concentrations were assessed by flow cytometry. One of the black colored lakes located in a landscape of rapidly degrading palsas (permafrost mounds) was selected for high-throughput 18S rRNA sequencing to help interpret the pigment and cytometry data. The results showed that the limnological properties of the thaw lakes differed significantly from the reference lakes, and were more highly stratified. However, both waterbody types contained similarly diverse phytoplankton groups, with dominance of the pigment assemblages by fucoxanthin-containing taxa, as well as chlorophytes, cryptophytes and cyanobacteria. Chlorophyll *a* concentrations (Chl *a*) were correlated with total phosphorus (TP), and both were significantly higher in the thaw lakes (overall means of 3.3 µg Chl *a* $L^{-1}$ and 34 µg TP $L^{-1}$) relative to the reference lakes (2.0 µg Chl *a* $L^{-1}$ and 8.2 µg TP $L^{-1}$). Stepwise multiple regression of Chl *a* against the other algal pigments showed that it was largely a function of lutein, fucoxanthin and peridinin ($R^2 = 0.78$). The bottom waters of two of the thaw lakes also contained high concentrations of bacteriochlorophyll *d*, showing the presence of green photosynthetic sulphur bacteria. The molecular analyses indicated a relatively minor contribution of diatoms, while chrysophytes, dinoflagellates and chlorophytes were well represented; the heterotrophic eukaryote





BGD
12, 12121–12156, 2015



fraction was dominated by numerous ciliate taxa, and also included Heliozoa, Rhizaria, chytrids and flagellates. Autotrophic picoplankton occurred in cell concentrations up to $8.8 \times 10^5$ mL$^{-1}$ (picocyanobacteria) and $4.6 \times 10^5$ mL$^{-1}$ (picoeukaryotes). Both groups of picophytoplankton were positively correlated with total phytoplankton abundance, as measured by Chl *a*; picocyanobacteria were inversely correlated with dissolved organic carbon, while picoeukaryotes were correlated with conductivity. Despite their net heterotrophic character, subarctic thaw lakes are rich habitats for diverse phototrophic communities.

## 1 Introduction

Degradation of ice-rich permafrost leads to the formation of thaw lakes, which are among the most abundant aquatic habitats in high latitude regions (Pienitz et al., 2008; Jones et al., 2012). These environments have attracted increasing scientific interest because of their biogeochemical reactivity. However, although there is rapidly increasing knowledge about their role in greenhouse gas (GHG) emissions (Laurion et al., 2010; Walter et al., 2006), little is known about their photosynthetic communities. Phototrophic organisms consume $CO_2$ and thereby reduce the net emission to the atmosphere; however, few studies have examined phytoplankton or other phototrophs in these abundant waters. Early studies in the US Tundra Biome Program at Barrow, Alaska, recorded 105 species of algae in tundra lakes and ponds, with dominance of cryptophytes and chrysophytes (Alexander et al., 1980). More recent studies have focused on thaw lake diatoms as paleolimnological indicators, but the dominants in these records are often benthic taxa such as *Pinnularia* and *Fragilaria* (Bouchard et al., 2013). A lake survey in the western Hudson Bay lowlands, including in permafrost catchments, showed that the phytoplankton had diverse communities, primarily composed of cyanobacteria, chrysophytes, chlorophytes, cryptophytes, dinoflagellates and diatoms (Paterson et al., 2014).





BGD
12, 12121–12156, 2015



Picophytoplankton (PP), consisting of picocyanobacteria and picoeukaryotes (nominally defined as cells 1 to 3 µm in diameter), contribute a major fraction of the total phototrophic biomass across a wide range of aquatic ecosystems (Richardson and Jackson, 2007), including northern lakes and rivers (Waleron et al., 2007; Vallières et al., 2008). In subarctic (Bergeron and Vincent, 1997) and high arctic (van Hove et al., 2008) lakes, picocyanobacteria may dominate the phytoplankton community in terms of biomass as well as cell abundance. For example, in large oligotrophic Clear Water Lake (Lac à l'Eau Claire, Nunavik, Canada), small cell phytoplankton (the cell fraction that passed through a 2 µm filter) accounted for 75 % of the total phytoplankton Chl *a* (Bergeron and Vincent, 1997). However, the suitability of permafrost thaw lakes as a habitat for picophytoplankton has not been explored.

Our overall aim in the present study was to evaluate by pigment analysis the major groups of phytoplankton in subarctic thaw lakes, and to relate this abundance and community structure to environmental variables. A secondary objective was to determine the abundance and distribution of picocyanobacteria and picoeukaryotes. As a further guide to the composition of the eukaryotic plankton, and in support of the pigment and picoplankton observations, we also applied high throughput 18S rRNA sequencing to surface and bottom waters from one selected lake that was strongly influenced by permafrost degradation. Our study included a wide range of small lakes across the gradient of permafrost degradation in Subarctic Quebec, Canada, from sporadic permafrost landscapes in the south (less than 10 % of the area containing permafrost) to discontinuous permafrost in the north (10–90 % permafrost). We also took comparative samples from a set of shallow rock-basin lakes that are unaffected by thermokarst processes. Given their limnological variability, as indicated by the variety of water colors among thaw lakes, we hypothesized that there would be large variations in total phytoplankton pigment concentration, pigment diversity and picophytoplankton abundance. Degrading permafrost soils release dissolved organic carbon (DOC) and fine inorganic particles into the thaw lakes, and these constituents attenuate light down the water column and determine the variability in color (Watanabe et al., 2011). DOC also





BGD
12, 12121–12156, 2015



influences the near surface thermal and stratification regime (Caplanne and Laurion, 2008), and temperature is known to exert a direct effect on phytoplankton community structure, particularly favouring cyanobacterial dominance (Paerl and Huisman, 2008). We therefore hypothesised that DOC and temperature would be the primary drivers of variations in phytoplankton pigmentation and picophytoplankton abundance.

## 2 Materials and methods

### 2.1 Study sites

Twelve thaw lakes (small perennial waterbodies created by thermokarst erosion of the permafrost) were sampled in subarctic Québec during the period of warm open-water conditions, in late summer (August) 2011 and 2012. The lakes were distributed along a north–south permafrost degradation gradient and across four geographically distinct locations: the Sasapimakwananisikw River valley (SAS) and the Kwakwatanikapistikw River valley (KWK) near Whapmagoostui-Kuujjuarapik; and the Sheldrake River valley (BGR) and the Nastapoka River valley (NAS) near Umiujaq. The KWK and SAS valleys occur within the sporadic permafrost landscape, while the BGR and NAS valleys are located in the discontinuous permafrost landscape (Fig. 1). Each valley is characterised by distinct vegetation cover and soil structure. Lakes located within the KWK valley are situated on impermeable clay-silt beds where the drainage basin is covered with dense shrub vegetation (Breton et al., 2009), whereas lakes in the SAS valley are located in peatlands in which permafrost mounds (palsas) are thawing and degrading rapidly (Bhiry et al., 2011). The lakes located in the northern valleys (BGR, NAS) are situated on marine clay-silt beds and are surrounded by forest and shrub tundra. In addition to permafrost thaw lakes, a set of five shallow rock-basin lakes (SRB) located on basalt bedrock was sampled in the vicinity of Whapmagoostui-Kuujjuarapik.





BGD
12, 12121–12156, 2015



## 2.2 Physicochemical analyses

Profiles of temperature, dissolved oxygen, conductivity, and pH of the 17 lakes were recorded with a 600R multiparametric probe (Yellow Springs Instrument Co.). Additionally temperature and conductivity were recorded with RBR XR620 conductivity-temperature-depth profiler (Richard Brancker Research Ltd). Near surface water samples (0.2 m depth) were collected into dark polyethylene bottles, previously washed with 10 % hydrochloric acid and rinsed in MQ water. The samples were stored in coolers and transported to laboratory within 4 h of collection. The total nitrogen (TN) and total phosphorus (TP) measurements were performed on unfiltered water samples collected in 125 mL bottles, acidified with sulfuric acid (0.2 % final concentration), and stored at 4 °C until persulfate digestion. TN concentrations were then measured with a Lachat flow injection analyzer and TP concentrations were measured using a Genesys 10 UV spectrophotometer (Thermo Spectronic) and standard techniques (Stainton et al., 1977). Total suspended solids (TSS) were collected onto pre-combusted and pre-weighed glass fiber filters (Advantec MFS) that were dried for 2 h at 60 °C and weighed on a Sartorius high precision balance. Dissolved organic carbon (DOC), colored dissolved organic matter (CDOM), soluble reactive phosphorus (SRP) and nitrate ($NO_3^-$) measurements were performed on water filtered through 0.2 µm cellulose acetate filters (Advantec MFS). Samples for DOC analyses were stored in 45 mL dark glass bottles that had been previously burned at 450 °C for 4 h and rinsed with MQ water to remove any traces of organic substances. The DOC analysis was with a Shimadzu TOC-5000A carbon analyzer calibrated with potassium biphthalate. CDOM was determined by spectrophotometric absorbance of the filtrates at 320 nm, blanked against filtered MQ water and converted to absorption values. SRP and $NO_3^-$ were measured in the filtrates using standard colorimetric methods (Stainton et al., 1977), and major ions were measured using Dionex ICS 2000 ion chromatograph.





BGD
12, 12121–12156, 2015



## 2.3 Pigment analysis

Surface and near-bottom water samples (50–500 mL) from each lake were filtered onto 25 mm diameter GF/F glass-fibre filters, and immediately frozen and stored at −80 °C until pigment extraction in methanol. Pigments were analyzed by high performance liquid chromatography (HPLC) following the protocols and standards described in Bonilla et al. (2005). For some of the statistical analyses, photoprotective pigments (canthaxanthin, diadinoxanthin, echininone, lutein, violaxanthin and zeaxanthin) were separated from light harvesting, photosynthetic pigments (alloxanthin, Chl *b*, fucoxanthin and peridinin) as in Bonilla et al. (2005).

## 2.4 Picophytoplankton enumeration

Unfiltered water samples were transferred to 5 mL Cryovials, fixed with glutaraldehyde (10 % final concentration) and stored at −80 °C until analysis for picophytoplankton abundance. The cells were enumerated using a Becton Dickinson flow cytometer (BD FacsCalibur), equipped with an argon laser. Analyses were done at the lowest flow rate (12 µL $min^{-1}$), using a solution of 1 µm diameter, yellow-green microspheres (Polysciences, Inc) as an internal standard. Bead concentrations in the calibration solution were controlled using TrueCountAbsolute counting tubes (BD biosciences). Picocyanobacteria and picoeukaryotes were distinguished based on their chlorophyll and phycoerythrin fluorescence. Detection of the two groups was performed by the comparison of flow cytograms where cells were discriminated based on their side scatter signals (SSC) and both red (FL3) and orange fluorescence (FL2) as well as FL3 vs. FL2. Given the low oxygen conditions observed in the bottom layers of the thaw lakes, samples were also analysed for green sulfur bacteria (FL3 vs. SCC). The cytograms were analyzed using the Cell Quest Pro software, with manual gating to discriminate the different populations. For the picophytoplankton biovolume estimates, the diameters of 20 cells of each group in a sample from thaw lake KWK12 were measured under epifluorescence microscopy at 1000× magnification, and were then converted





BGD
12, 12121–12156, 2015



to spherical biovolumes. The measured cell diameters (±SD) were 1.0 ± 0.2 µm for picocyanobacteria and 2.0 ± 0.5 µm for picoeukaryotes.

### 2.5 RNA sampling and analysis

Water samples from the surface and bottom of the black palsa lake SAS2A were first prefiltered through a 20 µm mesh to remove larger organisms and then filtered sequentially through a 3 µm pore size, 47 mm diameter polycarbonate filter (DHI) and a 0.2 µm Sterivex unit (Millipore) with a peristaltic pump. From 100 to 300 mL of water were filtered and the filtration was stopped after 2 h to minimize RNA degradation. The 3 µm filter for larger cells (L fraction) and the 0.2 µm filter for the smaller fraction (S fraction) were both preserved in RNAlater (Life Technologies) and then stored at −80 °C until extraction.

Samples were extracted with the AllPrep DNA/RNA Mini Kit (Qiagen). This protocol was modified by the addition of cross-linked polyvinylpyrrolidone (PVP, Alfa Aesar) (UV light sterilized) to a final concentration of 10 % before loading the samples onto the lysate homogenization column. For all samples, the extracted RNA was converted to cDNA immediately with the High Capacity cDNA Reverse Transcription Kit (Applied Biosystems-Ambion) and stored at −80 °C until analysis. The V4 region of the eukaryotic 18S rRNA that had been converted to cDNA was amplified using the 454 primers as described in Comeau et al. (2011). PCR was carried out in a total volume of 50 µL, the mixture contained HF buffer 1X (NEB), 0.25 µM of each primer, 200 µM of each dNTPs (Life Technology), 0.4 mg mL$^{-1}$ BSA (NEB), 1 U of Phusion High-Fidelity DNA polymerase (NEB) and 1 µL of template cDNA. Two more reactions with 5X and 10X diluted template were also carried out for each sample, to minimize potential primer bias. Thermal cycling began with an initial denaturation at 98 °C for 30 s, followed by 30 cycles of denaturation at 98 °C for 10 s, annealing at 55 °C for 30 s, extension at 72 °C for 30 s and a final extension at 72 °C for 270 s. The three dilution reactions were pooled and purified with a magnetic bead kit Agencourt AMPure XP (Beckman Coulter) and then quantified spectrophotometerically with the Nanodrop 1000 (Thermo





BGD
12, 12121–12156, 2015



Fisher Scientific). The amplicons were sequenced on 1/8 plates of the Roche 454 GS-FLX using the "PLUS" chemistry at the IBIS/Laval University, Plate-Forme d'Analyses Génomiques (Québec City, QC). Reads have been deposited in the NCBI short read archive as SRP060634.

Sequences were analysed using the UPARSE pipeline (Edgar, 2013). For quality filtering, the sequences were truncated at 245 bp to keep 50 % of the reads at the 0.5 expected error rate. Singletons as well as chimeras were then removed and operational taxonomic units (OTUs) were determined at the ≥ 98 % similarity level. These OTUs were classified using the mothur classifier (Schloss et al., 2009) with a 0.8 confidence threshold based on the SILVA reference database (Pruesse et al., 2007) modified to include sequences from our in-house, curated northern 18S rRNA gene sequence database. In order to compare samples, the OTU tables were each subsampled 100 times at 2200 reads, which corresponded to the lowest number of reads per sample minus 10 %; this subsampling used the command multiple_rarefaction_even_depth.py in Qiime (Caporaso et al., 2010). The most abundant and unclassified OTUs were subsequently submitted to a BLASTn search to the nr database in NCBI GenBank (http://blast.ncbi.nlm.nih.gov/Blast.cgi) to identify the nearest match.

### 2.6 Statistical analysis

The normal distribution of environmental variables was tested using the Kolmogorov–Smirnov test, and right-skewed variables were normalized by natural logarithm transformation. Given the order of magnitude differences in picophytoplankton abundances and pigment concentrations among samples, the HPLC and flow cytometry data were also normalized by logarithmic transformation. Correlations within and among the phytoplankton, pigment and environmental variables were tested by Pearson correlation analysis, with correction for multi-testing using the false discovery rate procedure as in Benjamini and Hochberg (1995). Statistical relationships among variables were also investigated by principal component analysis (PCA), stepwise multiple linear regression, cluster analysis and permutation MANOVA (PERMANOVA). Secondary cross-





BGD
12, 12121–12156, 2015



correlated variables were removed prior to these analyses, which were performed using Past 3.04 or Primer 6.

## 3 Results

### 3.1 Environmental heterogeneity

The thaw lakes spanned a wide range of environmental conditions, including water color and CDOM, with the latter strongly correlated with DOC ($R = 0.67$, $p < 0.0001$). The highest DOC concentrations (up to 17 mg $L^{-1}$) and CDOM (up to 117 $m^{-1}$) were recorded in the SAS lakes (Table 1). These waters were black in color and also had the lowest pH values (6.0–6.6). The highest total nutrient concentrations (up to 125 µg TP $L^{-1}$ and 4 mg TN $L^{-1}$) were recorded in lakes located within the KWK and NAS valleys, and the values were lowest in the shallow rock-basin waters (minima of 1.6 µg TP $L^{-1}$ and 0.1 mg TN $L^{-1}$). Nitrogen to phosphorus ratios varied greatly among the 17 lakes, from 4 to 131 (g $g^{-1}$), and total suspended solids were similarly variable, from 1 to 320 mg $L^{-1}$ (Table 1). The NAS valley waters contained especially high concentrations of suspended clay particles, producing an opaque milky appearance. Despite their shallowness and small size, the thaw lakes were highly stratified in terms of temperature and oxygen (Fig. 2), with anoxic bottom waters in the SAS and KWK lakes. Some had pronounced thermal gradients, with temperature differences up to 10 °C between the surface and bottom waters. In contrast, the reference lakes were only weakly stratified (Fig. 2).

Principal component analysis (PCA) of environmental variables for surface water samples yielded three components with eigenvalues larger than 1, and these collectively explained 66 % of the total variance (Fig. 3). The first component explained 31 % of the observed variance and was positively correlated with Chl *a*, TSS, TN and TP. The second component was positively correlated with DOC, TN, conductivity and $NO_3$, and negatively with temperature (Table S2).





BGD
12, 12121–12156, 2015



Cluster analysis of a set of 8 non-autocorrelated environmental variables (TSS, TN, TP, DOC, temperature, pH, conductivity, $NO_3$) showed some grouping of the lakes, specifically of the SAS waters (Supplement Fig. S1) and PERMANOVA analysis of these data yielded an F value of 4.60 ($p < 0.0001$). The subsequent pairwise analysis of sites showed that the SRB reference waters differed significantly from the KWK, SAS and BGR ($p = 0.0006$, 0.0186 and 0.0468, respectively), however the three sets of thaw lakes did not differ significantly from each other ($p = 0.10$ to 0.18).

### 3.2 Planktonic pigments

Phytoplankton abundance, as measured by Chl *a* concentrations, varied greatly among the waterbodies (Table 1), from 0.4 (SRB1) to 6.8 (KWK6) $\mu g\,L^{-1}$ in 2011 and from 0.2 (SRB1) to 9.1 (KWK1) $\mu g\,L^{-1}$ in 2012. There was also a small but significant difference in Chl *a* concentrations between years, with means of 3.7 and 2.6 $\mu g\,L^{-1}$, respectively (paired *t* test, $t = 2.5$, $p = 0.02$). On average, Chl *a* was significantly higher in the thaw lakes than the reference rock-basin waters: the overall means were 3.3 and 2.0 $\mu g$ Chl *a* $L^{-1}$, respectively.

The pigment analyses of the phytoplankton sampled in 2011 (Fig. 4, Table 2) showed that there were diverse communities including fucoxanthin-containing groups (potentially diatoms, chrysophytes and certain dinoflagellates), chlorophytes (Chl *b*, lutein and violaxanthin), cryptophytes (alloxanthin), dinoflagellates (peridinin) and cyanobacteria (zeaxanthin, canthaxanthin, echinenone). The KWK lakes had high concentrations of zeaxanthin (up to 1.3 $\mu g\,L^{-1}$), accompanied by high concentrations of fucoxanthin and green algal pigments (lutein and violaxanthin). In the SAS lakes, a dominance of dinoflagellates and cryptophytes was indicated by high concentrations of peridinin and alloxanthin. Echinenone was present in KWK and SRB lakes and high concentrations of violaxanthin were also recorded in BGR lakes.

The bottom waters of the thaw lakes also contained diverse planktonic pigments, including high levels of alloxanthin (KWK and BGR) and fucoxanthin (KWK, BGR and SAS). The bottom waters of the shallow rock-basin waters contained high fucoxanthin





BGD
12, 12121–12156, 2015



concentrations. Diadinoxanthin was abundant in the bottom waters at several sites, particularly those in the KWK valley. High levels of bacteriochlorophyll *d* indicating abundant populations of green photosynthetic sulfur bacteria were recorded in the deeper waters of KWK (Table 3, Fig. 5).

Similarly diverse pigment assemblages were observed in 2012 (Fig. 4, Table 2). The abundance of cyanobacterial populations in KWK, BGR and NAS lakes was indicated by high concentrations of zeaxanthin (e.g., NASH) and echinenone (SRB3). Green algal pigments were abundant in the KWK lakes as well as in some shallow rock-basin waters, and high diadinoxanthin concentrations appeared in KWK, SAS and BGR lakes. Fucoxanthin-groups were abundant in SRB and SAS as well as in NASH and BGR2. The turbid thaw lakes within the NAS valley had high concentrations of $\beta,\beta$-carotene. Relatively high levels of ancillary photosynthetic pigments were present in BGR and NAS lakes as well as in clear waters of shallow rock-basin lakes (Table 2). Photoprotective pigments were relatively more abundant in KWK lakes (notably KWK6 and KWK23) as well as in the SRB waters (violaxanthin), and less abundant in the DOC-rich SAS lakes (Table 2). The bottom waters contained high levels of diadinoxanthin and alloxanthin in KWK lakes, fucoxanthin in BGR2 and Chl *b* in SRB. Bacteriochlorophyll *d* was again present in the bottom and mid-water column of the KWK lakes that had anoxic bottom waters.

For the overall data set, Chl *a* concentrations were significantly correlated with TP ($R = 0.48$; $p = 0.05$), and with TSS ($R = 0.53$; $P = 0.03$), which were themselves strongly correlated ($R = 0.76$; $p < 0.0001$). A forward stepwise linear regression showed that Chl *a* was best described by a combination of the accessory pigments lutein ($p < 0.001$), fucoxanthin ($p = 0.003$) and peridinin ($p = 0.05$): $\ln \text{Chl } a = 1.57 \ln \text{Lut} + 0.58 \ln \text{Fuco} + 0.48 \ln \text{Per} + 0.48$ ($R^2 = 0.78$; $p < 0.001$). The regression analyses between principal components and accessory pigments showed a significant relationship for lutein and the first and second principal components: ($R^2 = 0.48$, $p = 0.001$), and zeaxanthin was significantly related to the third component ($R^2 = 0.26$, $p = 0.01$).





BGD
12, 12121–12156, 2015



Several of the accessory pigments were highly correlated among themselves. These included the chlorophyte pigments violaxanthin and lutein ($R = 0.82$; $p < 0.0001$), and both pigments with Chl *b* ($R = 0.66$, 0.90; $p = 0.0004$, $< 0.0001$). The cyanobacterial pigments echinenone and canthaxanthin were significantly correlated ($R = 0.70$; $p = 0.0001$), but not with zeaxanthin ($p > 0.1$). Diadinoxathin and violaxanthin were also strongly correlated ($R = 0.72$, $p < 0.001$). The summations within the two categories of pigments, photoprotective and photosynthetic, were also positively correlated ($R = 0.73$; $p < 0.001$).

PERMANOVA analysis was conducted on a data subset of 5 non-autocorrelated accessory pigments: fucoxanthin, peridinin, lutein, echinenone and zeaxanthin. These showed no significant differences among valleys ($F = 1.34$, $p = 0.172$). Similarly, cluster analysis showed no grouping of pigment characteristics according to site, although there was some evidence of grouping according to sample year (Fig. S2). The mapping of this cluster matrix on the environmental cluster matrix via the Primer function Relate showed no significant relationship ($R = -0.23$, $p = 0.10$).

Consistent with the multivariate analyses, the accessory pigments were uncorrelated with individual environmental variables (all corrected *p* values were > 0.05), with the exception of lutein. This chlorophyte pigment was significantly correlated with TP ($R = 0.49$; $p = 0.05$), but this may simply reflect the strong correlation between lutein and Chl *a* ($R = 0.79$; $p < 0.0001$), which itself correlated with TP (see above).

### 3.3 Picophytoplankton abundance

Picophytoplankton concentrations varied greatly among the lakes (Fig. 6). In 2011, those located on marine clays (KWK) contained the highest abundance of total picophytoplankton. The picocyanobacterial abundances ranged from $4.2 \times 10^2$ (SAS1) to $5.6 \times 10^5$ cells mL$^{-1}$ (KWK23). The BGR lakes also contained abundant picophytoplankton, but with lower contributions from picoeukaryotes. The thaw lakes located on peatlands (SAS) contained up to $10^5$ cells mL$^{-1}$ of total picophytoplankton with prevalence of picoeukaryotes over picocyanobacteria. The smaller rock-basin lakes





BGD
12, 12121–12156, 2015



(SRB1, SRB2, SRB4) contained up to $10^4$ picophytoplankton cells $mL^{-1}$ and two larger rock-basin lakes (SRB3, SRB5) contained up to $10^5$ picophytoplankton cells $mL^{-1}$, with high contributions from picocyanobacteria. In 2012, the picophytoplankton populations reached $10^6$ cells $mL^{-1}$ in KWK lakes, with the highest numbers of picocyanobacteria, reaching $8.8 \times 10^5$ cells $mL^{-1}$ in KWK1. The highest numbers of picoeukaryotes were also recorded in KWK1, with concentrations up to $4.6 \times 10^5$ cells $mL^{-1}$ in 2011. The shallow rock-basin (SRB) and peatland lakes (SAS) were apparently less favourable, with picoeukaryote concentrations below $10^3$ cells $mL^{-1}$. The lower abundances of picoeukaryotes were not always accompanied by similar decrease in picocyanobacteria, for example in SRB3.

Total picophytoplankton abundance increased with Chl *a* concentration ($R = 0.52$; $p = 0.03$), but this relationship was only significant for the eukaryotic component ($R = 0.53$; $p = 0.02$). Picocyanobacteria correlated negatively with DOC ($R = -0.47$; $p = 0.05$), while picoeukaryotes correlated negatively with conductivity ($R = -0.48$; $p = 0.05$). Picocyanobacteria were highly correlated with zeaxanthin ($R = 0.72$; $p = 0.0002$), and there was also a significant, albeit less strong, correlation between picoeukaryotes and zeaxanthin ($R = 0.54$; $p = 0.02$). Stepwise multiple linear regression analysis showed that picophytoplankton (picoeukaryotes, PEuk; picocyanobacteria, PCyan) abundances were statistically related to limnological variables according to the relationships: PEuk = 14.9 + 2.9× Chl *a* – 1.7 × TN ($R^2 = 0.56$, $p = 0.001$), and PCyan = −2.9 + 4.3 Temp + 1.1× Chl *a* – 1.1 × TSS + 1.5 × TP – 1.2 × DOC ($R^2 = 0.67$, $p = 0.001$).

### 3.4 Molecular analyses

The 18S rRNA data set from the palsa thaw lake (SAS2A) contained large numbers of rotifer sequences (400 to 1350 reads per sample, all with closest matches to the genus *Ascomorpha*) and these were removed prior to further analysis. This left a total of 3857 and 3128 reads for the surface L (> 3.0 µm) and S (< 3.0 µm) fractions, and





BGD
12, 12121–12156, 2015



3522 and 2457 reads for the bottom L and S fractions, 84 to 93 % of these eukaryotic sequences could be assigned (≥ 98 % identity) to phylum in the modified SILVA database. The largest fraction of total reads was attributable to ciliates (up to 33 % in the surface waters and 74 % in the bottom waters; Table 4), including the genus *Stokesia,* especially in the surface waters, and the genera *Cryptocaryon, Halteria*, *Peniculida* and *Cyclidium*, especially in the bottom waters (Table 5). Among the groups nominally considered as phytoplankton were dinoflagellates, chrysophytes and chlorophytes, with lesser proportions of reads associated with katablepharids, bacillariophytes (diatoms) and cryptophytes (Table 4). Cluster analysis of the data set (after subsampling to ensure equal reads per fraction and water depth) showed that community structure greatly differed with depth (Bray–Curtis dissimilarity index of 0.795 for the large fraction and 0.820 for the small fraction), and to a much lesser extent between large and small fractions (Bray–Curtis dissimilarity index of 0.423 for the surface samples and 0.312 for the bottom samples). Chlorophytes, dinoflagellates, katablepharids and diatoms were more represented in the large, surface water fraction.

## 4 Discussion

Each of the subarctic thaw lakes contained pigments from several phytoplankton phyla, revealing that these abundant waters provide habitats for diverse phototrophic groups. Apart from $\beta$,$\beta$-carotene found in all algal groups, the most abundant accessory pigment was fucoxanthin, indicating the prevalence of diatoms, chrysophytes and possibly certain dinoflagellates. Peridinin and alloxanthin were also present in many of the samples, indicating the presence of dinoflagellates and cryptophytes, respectively (Jeffrey et al., 2011). Diatoms would be less favoured in these stratified waters given their fast sinking rates in still waters, while flagellated taxa including chrysophytes, dinoflagellates and cryptophytes would be able to maintain their position in the euphotic zone. Mixotrophic chrysophytes and dinoflagellates have been observed in many high latitude lakes (Charvet et al., 2012; and references therein), and may be additionally fa-





BGD
12, 12121–12156, 2015



vored by the high biomass concentrations of heterotrophic bacteria that occur in some of these waters (Breton et al., 2009; Roiha et al., 2015). Green algae were also well represented at most sites, indicating that despite the strong light attenuation by CDOM and TSS in these waters (Watanabe et al., 2011), there is adequate light availability for obligate phototrophs; some of these taxa, however, may also be capable of osmotrophic uptake of dissolved organic compounds.

The concentrations of photoprotective pigments, in particular $\beta$,$\beta$-carotene, were conspicuously high in the NAS lakes. This was unexpected given that these turbid waters contained elevated concentrations of suspended solids, which indicate a low light availability for photosynthesis, and a lack of need for protection against bright light. It is possible, however, that in this lake, cells suspended in the mixed layer are adapted to intermittent exposure to bright light rather than the average water column irradiance. Such conditions have been observed in a turbid estuarine environment, where the phytoplankton were photosynthetically adapted to high near-surface irradiances rather than the overall shade or dark conditions experienced on average by the cells as they were circulated by turbulent mixing through the water column (Vincent et al., 1994).

The pigment analyses also indicated the abundant presence of cyanobacteria. Echinenone and canthaxanthin are well known photoprotective pigments in cyanobacteria, with the latter especially prevalent in Nostocales, which may suggest the presence of nitrogen-fixing taxa. These results are consistent with bacterial 16S rRNA analyses, which showed the presence of cyanobacterial taxa in some of these lakes that had strong affinities (> 99 % sequence similarity) to the Nostocalean taxon *Dolichospermum curvum* (Crevecoeur et al., 2015). Zeaxanthin can occur in high cellular concentrations in picocyanobacteria, but it also is found in several eukaryotic algal groups. This pigment is a component of photoprotective xanthophyll cycles, and may co-occur with other components of these cycles. For example, studies on the diatom *Phaedactylum tricornutum* have shown the co-occurrence of the diadinoxanthin cycle and the violaxanthin cycle (Lohr and Wilhelm, 1999). Consistent with this co-occurrence, we found a strong correlation between diadinoxanthin and violaxanthin in the studied lakes





BGD
12, 12121–12156, 2015



($R = 0.72$, $p < 0.001$). We also observed high concentrations of zeaxanthin, which is often associated with cyanobacteria but also chlorophytes (Jeffrey et al., 2011). Given the molecular analyses results of thaw lake bacterial communities (Crevecoeur et al., 2015) and our flow cytometry data, zeaxanthin was likely to at least in part be associated with the abundant picocyanobacteria in the order Synechococcales. The strong correlation between picocyanobacteria and zeaxanthin further supports this relationship.

HPLC analysis has been used with success in a variety of aquatic ecosystems to not only identify major algal groups, but also to quantify their proportional representation using the software program CHEMTAX (Mackay et al., 1996). However, given the large known variation in pigment ratios in algal cells, this method requires extensive calibration on each class of waters. For example, in shallow lake, CHEMTAX gave a reliable estimation of cyanobacterial and chlorophyte biomass, but not chrysophytes and dinoflagellates (Tamm et al., 2015). The latter were two of the dominant groups in the permafrost thaw lakes, and further work will be required before the CHEMTAX approach can be applied to these waters.

The presence of bacteriochlorophyll *d* in high concentrations in KWK lakes containing anoxic bottom waters indicate that these environments are favourable habitats for photosynthetic sulfur bacteria. These results are consistent with molecular analyses of the bacterial assemblages. 16S rRNA gene clone library analysis of KWK lakes detected the presence of green sulfur bacteria (Rossi et al., 2013), and high throughput 16S rRNA sequencing revealed that the green sulfur bacterium *Pelodictyon* (Chlorobi) was one of the most abundant sequences in KWK waters (Crevecoeur et al., 2015). The high concentrations of bacteriochlorophyll *d* suggest that these populations could play an important role in overall primary production of certain thaw lakes, although restricted to deeper water, anoxic conditions.

Picophytoplankton occurred in all of the sampled lakes, but with large differences among waters. In general, the concentrations of both picocyanobacteria and picoeukaryotes increased with increasing total phytoplankton biomass, as measured by





BGD
12, 12121–12156, 2015



Chl *a* concentrations. However, the two groups differed in their correlative relationships with other limnological variables. In partial support of our initial hypothesis that DOC would be a controlling variable, picocyanobacteria, but not eukaryotes, were negatively correlated with DOC. An inverse relationship with DOC was also found for picophytoplankton in Swedish lakes (Drakare et al., 2003). Similarly in Lake Valkea-Kotinen, in the boreal zone of Finland, variations in autotrophic picoplankton were most closely correlated with water column stability, which in turn was strongly regulated by DOC concentration (Pelromaa and Ojala, 2012). High DOC waters are often characterized by low pH, which may be a constraint on certain cyanobacteria, however acid-tolerant picocyanobacteria are known (Jasser et al., 2013). Even in the low pH SAS waters picocyanobacteria were always present, although in low concentrations (e.g., the minimum of $1.8 \times 10^3$ m L$^{-1}$ in SAS2B in 2011). Other factors such as zooplankton grazing may also have played a role in controlling picocyanobacteria (Rautio and Vincent, 2006), although this seems less likely for picocyanobacteria given that they are a nutritionally deficient food source for zooplankton in thaw lakes (Przytulska et al., 2015).

Picocyanobacteria did not show the expected relationship with temperature in the correlation analyses, although temperature was one of the variables retained in the multiple linear regression analysis. Temperature has often been identified as a key variable for cyanobacterial growth and dominance in lakes elsewhere. For example, in reservoirs in the southeastern USA, there was a strong, positive correlation between picocyanobacterial cell concentrations and temperature, while picoeukaryotes showed an inverse correlation, and dominance of the picophytoplankton community shifted from picoeukaryotes in winter to picocyanobacteria in summer (Ochs and Rhew, 1997). Similarly, increasing temperature favoured picocyanobacteria over picoeukaryotes in German lakes (Hepperle and Krienitz, 2001). In experiments with subarctic lake and river water at 10 and 20 °C, the concentration of Chl *a* in the picoplankton fraction increased substantially at the warmer temperature (Rae and Vincent, 1998). The temperature range in the present study may have been too restricted to observe such effects.





BGD
12, 12121–12156, 2015



The molecular data provided further insight into the planktonic diversity of a thaw lake ecosystem. The RNA sequences in SAS2A were dominated by ciliates, likely reflecting their large cell sizes with a concomitantly large number of ribosomes; for example, *Stokesia vernalis,* the most abundant sequence identified in the surface waters (Table 5), can be > 100 µm in length. Ciliates are also known to be fragile cells that are easily broken up during manipulation (pre-filtration through a 20 µm mesh), likely accounting for their highly abundant sequences in the S as well as L fractions. Chrysophytes and chlorophytes were well represented in the RNA sequences, particularly in the surface water L fraction, consistent with their abundance as indicated by the pigment data. Dinoflagellates constituted the dominant fraction of the phytoplankton sequences, yet were not detected as peridinin in SAS2A, although this pigment was present in two other SAS lakes. This may indicate the presence of large dinoflagellate cells, for example rigid *Ceratium* cells that can extend up to 100 µm in length, but may also be due to the presence of dinoflagellates that lack the accessory pigment peridinin. Diatoms can also include large cell types, but their representation in the sequences was small, suggesting that most of the fucoxanthin that we measured was associated with chrysophytes such as *Uroglena* (Table 5) rather than diatoms. It is of interest that diatoms from the genus *Urosolenia* were the closest match following a BLAST search. This diatom is known to be lightly silicified and may be less susceptible to sedimentation in these well stratified waters. The cryptophyte pigment alloxanthin was in high concentration in SAS2A, as in the other thaw lakes, yet cryptophyte sequences accounted for < 1.5 % of the total RNA reads. This might reflect the small cell-size and accordingly low rRNA content of certain cryptophyte taxa, for example *Chroomonas*.

The molecular data also provided insight into the nature of the picoeukaryotic communities in the SAS lakes. The taxonomic identities (Table 5) indicated the presence of several chlorophyte genera that are known to produce small cells, notably *Choricystis*, *Lemmermannia Monoraphidium* and *Chlorella*. For example, in subalpine Lake Tahoe (USA), *Choricystis coccoides* produces cells that are only 0.5 µm$^3$ in volume, too small to be grazed by calanoid copepods in that lake (Vincent, 1982). Among the chryso-





BGD
12, 12121–12156, 2015



phytes, *Spumella* and related genera are known to produce small cells. For all of these analyses, the many unidentified eukaryotic reads add an extra element of uncertainty to the interpretation, but collectively these data underscore the planktonic diversity of the thaw lake ecosystem.

Permafrost thaw lakes receive large quantities of allochthonous organic carbon from their surrounding catchments and this is reflected in their high DOC and CDOM concentrations, as observed in the present study. These waters have high respiratory oxygen demands and are net heterotrophic, resulting in prolonged hypoxia or anoxia in the bottom waters during summer, and anoxia throughout the water column once ice covers the lake in winter (Deshpande et al., 2015). The abundant cilate and nanoflagellate sequences in our molecular analyses also point to high productivity by bacterial heterotrophs, their likely prey in these waters. However, despite these multiple signs of intense heterotrophy, the pigment, cytometry and molecular results in the present study show that these ecosystems are also the habitats for abundant phototrophs from diverse taxonomic groups.

## 5 Conclusions

The thaw lakes sampled in the present study significantly differed from the reference rock basin lakes in their limnological properties. On average, they contained higher phytoplankton (Chl *a*) and TP concentrations than the reference lakes, but had a comparable diversity of pigments, dominated by chlorophyte, chrysophyte and dinoflagellate pigments. Cyanobacteria and cryptophytes were also well represented, but the thaw waters appeared to be less favorable for diatoms, at least during the highly stratified late-summer period. Picophytoplankton occurred in all of the thaw lakes, in some of the waters at high abundances up to $10^6$ cells $mL^{-1}$, and the molecular analysis indicated that small cell chlorophytes may be among the dominants in the picoeukaryotic fraction. Despite the heterotrophic nature of these organic-rich ecosystems, with respiration likely exceeding photosynthesis throughout the year, permafrost thaw lakes





BGD
12, 12121–12156, 2015



contain abundant, diverse phototrophs that potentially support higher trophic levels, and that will lessen the net $CO_2$ release from these waters to the atmosphere.

**The Supplement related to this article is available online at doi:10.5194/bgd-12-12121-2015-supplement.**

*Author contributions.* A. Przytulska, W. F. Vincent and I. Laurion designed the study; A. Przytulska led the field sampling; S. Crevecoeur with input from J. Comte undertook the molecular analyses under the supervision of C. Lovejoy; laboratory analyses were overseen by A. Przytulska, W. F. Vincent and I. Laurion; flow cytometry analyses were by J. Comte and A. Przytulska, under the supervision of I. Laurion; and data analysis was by A. Przytulska with input from J. Comte, S. Crevecoeur and W. F. Vincent. A. Przytulska prepared the manuscript with contributions from all co-authors.

*Acknowledgements.* We thank Marie-Josée Martineau for laboratory assistance with the HPLC analyses, and ADAPT colleagues Paschale Bégin, Bethany Deshpande and Alex Matveev, for assistance in the field. We are also grateful to Maciek Bartosiewicz for his help throughout this project and Adam Monier for aid with bioinformatics advice. This study was funded by the Natural Sciences and Engineering Research Council of Canada (NSERC) including the Discovery Frontiers ADAPT grant to W. F. Vincent and an EnviroNord fellowship to J. Comte, Fonds de recherche du Québec, the Network of Centres of Excellence ArcticNet and the Canada Research Chair program.

## References

Alexander, V., Stanley, D. W., Daley, R. J., and McRoy, C. P.: Primary producers, in: Limnology of Tundra Ponds, Barrow, Alaska, edited by: Hobbie, J. E., Dowden, Hutchinson, Ross Inc, Stroudsburg, PA, U.S./IBP synthesis series, 13, 179–250, 1980.

Benjamini, Y. and Hochberg, Y.: Controlling the false discovery rate: a practical and powerful approach to multiple testing, J. Roy. Stat. Soc. B, 57, 289–300, 1995.





BGD
12, 12121–12156, 2015



Bergeron, M. and Vincent, W. F.: Microbial food web responses to phosphorus and solar UV radiation in a subarctic lake, Aquat. Microb. Ecol., 12, 239–249, 1997.
Bhiry, N., Delwaide, A., Allard, M., Bégin, Y., Filion, L., Lavoie, M., Nozais, C., Payette, S., Pienitz, R., Saulnier-Talbotb, E., and Vincent, W. F.: Environmental change in the Great Whale River region, Hudson Bay: five decades of multidisciplinary research by Centre d'études nordiques (CEN), Ecoscience, 18, 182–203, doi:10.2980/18-3-3469, 2011.
Bonilla, S., Villeneuve, V., and Vincent, W. F.: Benthic and planktonic algal communities in a high arctic lake: pigment structure and contrasting responses to nutrient enrichment, J. Phycol., 41, 1120–1130, doi:10.1111/j.1529-8817.2005.00154.x, 2005.
Bouchard, F., Pienitz, R., Ortiz, J. D., Francus, P., and Laurion, I.: Palaeolimnological conditions inferred from fossil diatom assemblages and derivative spectral properties of sediments in thermokarst ponds of subarctic Quebec, Canada, Boreas, 42, 575–595, doi:10.1111/bor.12000, 2013.
Breton, J., Vallières, C., and Laurion, I.: Limnological properties of permafrost thaw ponds in northeastern Canada, Can. J. Fish. Aquat. Sci., 66, 1635–1648, doi:10.1139/F09-108, 2009.
Caplanne, S. and Laurion, I.: Effects of chromophoric dissolved organic matter on epilimnetic stratification in lakes, Aquat. Sci., 70, 123–133, doi:10.1007/s00027-007-7006-0, 2008.
Caporaso, J. G., Kuczynski, J., Stombaugh, J., Bittinger, K., Bushman, F. D., Costello, E. K., and Fierer, N.: Qiime allows analysis of high-throughput community sequencing data, Nat. Methods, 7, 335–336, doi:10.1038/nmeth.f.303, 2010.
Charvet, S., Vincent, W. F., and Lovejoy, C.: Chrysophytes and other protists in high Arctic lakes: molecular gene surveys, pigment signatures and microscopy, Polar Biol., 35, 733–748, doi:10.1007/s00300-011-1118-7, 2012.
Comeau, A. M., Li, W. K. W., Tremblay, J. É., Carmack, E. C., and Lovejoy, C.: Arctic Ocean microbial community structure before and after the 2007 record sea ice minimum, PloS ONE, 6, e27492, doi:10.1371/journal.pone.0027492, 2011.
Crevecoeur, S., Vincent, W. F., Comte, J., and Lovejoy, C.: Bacterial community structure across environmental gradients in permafrost thaw ponds: methanotroph-rich ecosystems, Front. Microbiol., 6, 192, doi:10.3389/fmicb.2015.00192, 2015.
Deshpande, B. N., MacIntyre, S., Matveev, A., and Vincent, W. F.: Oxygen dynamics in permafrost thaw lakes: anaerobic bioreactors in the Canadian subarctic, Limnol. Oceanogr., 60, doi:10.1002/lno.10126, 2015.





BGD
12, 12121–12156, 2015



Drakare, S., Blomqvist, P., Bergström, A. K., and Jansson, M.: Relationships between picophytoplankton and environmental variables in lakes along a gradient of water colour and nutrient content, Freshwater Biol., 48, 729–740, doi:10.1046/j.1365-2427.2003.01049.x, 2003.
Edgar, R. C.: UPARSE: highly accurate OTU sequences from microbial amplicon reads, Nat. Methods,10, 996–998, doi:10.1038/nmeth.2604, 2013.
Hepperle, D. and Krienitz, L.: Systematics and ecology of chlorophyte picoplankton in German inland waters along a nutrient gradient, Int. Rev. Hydrobiol., 86, 269–284, 2001.
Jasser, I., Karnkowska-Ishikawa, A., and Chróst, R. J.: Do acid-tolerant picocyanobacteria exist? A study of two strains isolated from humic lakes in Poland, Hydrobiologia, 707, 209–218, doi:10.1007/s10750-012-1428-y, 2013.
Jeffrey, S. W., Wright, S. W., and Zapata, M.: Microalgal classes and their signature pigments, in: Phytoplankton Pigments: Characterization, Chemotaxonomy and Aplications in Oceanography, edited by: Roy, S., Llewellyn, C. A., Skarstad Egeland, E., and Johnsen, G., Cambridge University Press, UK, 52–53, 2011.
Jones, M., Grosse, G., Jones, B. M., and Walter Anthony, K. M.: Peat accumulation in a thermokarst-affected landscape in continuous ice-rich permafrost, Seward Peninsula, Alaska, J. Geophys. Res., 117, G00M07, doi:10.1029/2011JG001766, 2012.
Mackey, M. D., Mackey, D. J., Higgins, H. W., and Wright, S. W.: CHEMTAX – a program for estimating class abundances from chemical markers: application to HPLC measurements of phytoplankton, Mar. Ecol.-Prog. Ser., 144, 265–83, doi:10.3354/meps144265, 1996.
Laurion, I., Vincent, W. F., MacIntyre, S., Retamal, L., Dupont, C., Francus, P., and Pienitz, R.: Variability in greenhouse gas emissions from permafrost thaw ponds, Limnol. Oceanogr., 55, 115–133, doi:10.4319/lo.2010.55.1.0115, 2010.
Lohr, M. and Wilhelm, C.: Algae displaying the diadinoxanthin cycle also possess the violaxanthin cycle, P. Natl. Acad. Sci. USA, 96, 8784–8789, 1999.
Ochs, C. A. and Rhew, K.: Population dynamics of autotrophic picoplankton in a southeastern US reservoir, Int. Rev. Hydrobiol. Hydrogr., 82, 293–313, 1997.
Paerl, H. W. and Huisman, J.: Blooms like it hot, Science, 320, 57–58, doi:10.1126/science.1155398, 2008.
Paterson, A. M., Keller, W., Rühland K. M., Jones, C. F., and Winter, J. G.: An exploratory survey of summer water chemistry and plankton communities in lakes near the Sutton river, Hudson Bay lowlands, Ontario, Canada, Arct. Antarct. Alp. Res., 46, 121–138, doi:10.1657/1938-4246-46.1.121, 2014.





BGD
12, 12121–12156, 2015



Peltomaa, E. and Ojala, A.: Meteorological drivers of the dynamics of autotrophic picoplankton, Freshwater Biol., 57, 1005–1016, doi:10.1111/j.1365-2427.2012.02761.x, 2012.
Pienitz, R., Doran, P. T., and Lamoureux, S. F.: Origin and geomorphology of lakes in the polar regions. Polar lakes and rivers, limnology of Arctic and Antarctic aquatic ecosystems, Oxford University Press, Oxford, UK, 25–41, 2008.
Pruesse, E., Quast, C., Knittel, K., Fuchs, B. M., Ludwig, W., Peplies, J., and Glockner, F. O.: SILVA: a comprehensive online resource for quality checked and aligned ribosomal RNA sequence data compatible with ARB, Nucleic Acids Res., 35, 7188–7196, doi:10.1093/nar/gkm864, 2007.
Przytulska, A., Bartosiewicz, M., Rautio, M., Dufresne, F., and Vincent, W. F.: Climate effects on high latitude *Daphnia* via food quality and thresholds, PLoS ONE, 10, e0126231, doi:10.1371/journal.pone.0126231, 2015.
Rae, R. and Vincent, W. F.: Effects of temperature and ultraviolet radiation on microbial foodweb structure: potential responses to global change, Freshwater Biol., 40, 747–758, doi:10.1046/j.1365-2427.1998.00361.x, 1998.
Rautio, M. and Vincent, W. F.: Benthic and pelagic food resources for zooplankton in shallow high latitude lakes and ponds, Freshwater Biol., 51, 1038–1052, doi:10.1111/j.1365-2427.2006.01550.x, 2006.
Richardson, T. L. and Jackson, G. A.: Small phytoplankton and carbon export from the surface ocean, Science, 315, 838–840, doi:10.1126/science.1133471, 2007.
Roiha, T., Laurion, I., and Rautio, M.: Carbon dynamics in highly heterotrophic subarctic thaw ponds, Biogeosciences Discuss., 12, 11707–11749, doi:10.5194/bgd-12-11707-2015, 2015.
Rossi, P., Laurion, I., and Lovejoy, C.: Distribution and identity of bacteria in subarctic permafrost thaw ponds, Aquat. Microb. Ecol., 69, 231–245, doi:10.3354/ame01634, 2013.
Schloss, P. D., Westcott, S. L., Ryabin, T., Hall, J. R., and Hartmann, M.: Introducing mothur: open-source, platform-independent, community-supported software for describing and comparing microbial communities, Appl. Environ. Microb., 75, 7537–7541, doi:10.1128/AEM.01541-09, 2009.
Stainton, M., Capel, M., and Armstrong, F.: The Chemical Analysis of Fresh Water, 2nd edn., Special Publication 25, Canada Fisheries and Marine Service, Canada, 1977.
Tamm, M., Freiberg, R., Tõnno, I., Nõges, P., and Nõges, T.: Pigment-based chemotaxonomy – a quick alternative to determine algal assemblages in large shallow eutrophic lake?, PLoS ONE, 10, e0122526, doi:10.1371/journal.pone.0122526, 2015.





BGD
12, 12121–12156, 2015



Vallières, C., Retamal, L., Ramlal, P., Osburn, C. L., and Vincent, W. F.: Bacterial production and microbial food web structure in a large arctic river and the coastal Arctic Ocean, J. Marine Syst., 74, 756–773, doi:10.1016/j.jmarsys.2007.12.002, 2008.

Van Hove, P., Vincent, W. F., Galand, P. E., and Wilmotte, A.: Abundance and diversity of picocyanobacteria in high arctic lakes and fjords, Algological Studies, 126, 209–227, doi:10.1127/1864-1318/2008/0126-0209, 2008.

Vincent, W. F.: The autecology of an ultraplanktonic shade alga in Lake Tahoe, J. Phycol., 18, 226–232, 1982.

Vincent, W. F., Bertrand, N., and Frenette, J.-J.: Photoadaptation to intermittent light across the St. Lawrence Estuary freshwater-saltwater transition zone, Mar. Ecol.-Prog. Ser., 110, 283–292, 1994.

Waleron, M., Waleron, K., Vincent, W. F., and Wilmotte, A.: Allochthonous inputs of riverine picocyanobacteria to coastal waters in the Arctic Ocean, FEMS Microbiol. Ecol., 59, 356–365, doi:10.1111/j.1574-6941.2006.00236.x, 2007.

Walter, K. M., Zimov, S. A., Chanton, J. P., Verbyla, D., and Chapin III, F. S.: Methane bubbling from Siberian thaw lakes as a positive feedback to climate warming, Nature, 443, 71–75, doi:10.1038/nature05040, 2006.

Watanabe, S., Laurion, I., Chokmani, K., Pienitz, R., and Vincent, W. F.: Optical diversity of thaw ponds in discontinuous permafrost: a model system for water color analysis, J. Geophys. Res.-Biogeo., 116, G02003, doi:10.1029/2010JG001380, 2011.





BGD
12, 12121–12156, 2015



**Table 1.** Limnological characteristics including surface values for temperature ($T$), pH, dissolved organic carbon concentration (DOC), colored dissolved organic matter (CDOM), total suspended solids (TSS), soluble reactive phosphorus (SRP), total phosphorus (TP), total nitrogen (TN), nitrate ($NO_3$) and Chlorophyll *a* (Chl *a*) in studied subarctic lakes. Mean values from 2011 and 2012 (± range in brackets; nd = no data from 2011).

| Sites | $T$ (°C) | pH | DOC ($mg L^{-1}$) | CDOM ($m^{-1}$) | TSS ($mg L^{-1}$) | SRP ($\mu g L^{-1}$) | TP ($\mu g L^{-1}$) | TN ($mg L^{-1}$) | $NO_3$ ($mg L^{-1}$) | Chl *a* ($\mu g L^{-1}$) |
|---|---|---|---|---|---|---|---|---|---|---|
| Thaw lakes on marine clays | | | | | | | | | | |
| BGR1 | 15.1 (0.7) | 7.5 (0.2) | 3.9 (0.4) | 6.1 (1.7) | 2.9 (0.5) | 1.8 (0.6) | 17.3 (3.5) | 0.1 (0.0) | 0.05 (0.0) | 1.8 (1.0) |
| BGR2 | 14.5 (0.4) | 7.0 (0.3) | 9.0 (0.3) | 39.1 (5.7) | 19.2 (6.1) | 2.4 (1.0) | 45.7 (0.2) | 0.3 (0.0) | 0.05 (0.0) | 3.4 (1.4) |
| NASA | 15.6 (nd) | 7.0 (nd) | 3.0 (nd) | 12.3 (nd) | 319.3 (nd) | 2.9 (nd) | 124.5 (nd) | 3.7 (nd) | 0.25 (nd) | 4.1 (nd) |
| NASH | 18.3 (nd) | 7.6 (nd) | 4.1 (nd) | 22.6 (nd) | 18.2 (nd) | 6.2 (nd) | 28.5 (nd) | 0.4 (nd) | 0.04 (nd) | 1.7 (nd) |
| Thaw lakes on mineral clays | | | | | | | | | | |
| KWK1 | 17.1 (4.4) | 6.1 (0.8) | 9.2 (2.8) | 39.0 (16.4) | 14.1 (12.0) | 2.2 (1.5) | 36.8 (26.7) | 0.3 (0.1) | 0.05 (0.0) | 8.0 (1.2) |
| KWK6 | 14.9 (0.8) | 6.8 (0.4) | 5.2 (0.0) | 10.7 (0.7) | 9.3 (1.1) | 1.0 (0.4) | 30.9 (3.0) | 0.2 (0.0) | 0.06 (0.0) | 4.4 (1.6) |
| KWK12 | 16.8 (0.8) | 8.0 (1.1) | 8.6 (0.7) | 39.6 (3.7) | 13.8 (2.6) | 1.6 (0.0) | 27.7 (2.1) | 0.2 (0.0) | 0.08 (0.0) | 2.5 (0.1) |
| KWK23 | 14.9 (0.2) | 6.7 (0.2) | 7.2 (0.6) | 35.8 (1.9) | 10.2 (1.9) | 4.9 (0.6) | 47.7 (5.6) | 0.2 (0.0) | 0.04 (0.0) | 3.5 (1.9) |
| Thaw lakes on peatlands | | | | | | | | | | |
| SAS1A | 14.3 (0.2) | 6.6 (0.3) | 10.7 (0.8) | 68.7 (2.7) | 7.6 (2.6) | 1.6 (0.3) | 14.3 (0.9) | 0.5 (0.1) | 0.17 (0.0) | 3.6 (1.2) |
| SAS1B | 13.6 (0.1) | 6.3 (0.3) | 15.9 (0.4) | 109.5 (3.9) | 21.8 (5.4) | 1.9 (0.4) | 12.7 (2.2) | 0.6 (0.1) | 0.07 (0.0) | 4.3 (0.1) |
| SAS2A | 19.9 (nd) | 6.2 (nd) | 14.9 (nd) | 98.4 (nd) | 2.6 (nd) | 3.1 (nd) | 9.6 (nd) | 0.7 (nd) | 0.04 (nd) | 1.2 (nd) |
| SAS2B | 16.0 (nd) | 6.0 (nd) | 17.1 (nd) | 116.9 (nd) | 5.2 (nd) | 1.3 (nd) | 10.3 (nd) | 0.5 (nd) | 0.11 (nd) | 0.9 (nd) |
| Shallow rocky basins | | | | | | | | | | |
| SRB1 | 15.8 (2.2) | 7.6 (0.6) | 9.9 (0.0) | 46.0 (6.5) | 2.6 (1.2) | 2.1 (0.6) | 7.9 (2.8) | 0.2 (0.1) | 0.06 (0.0) | 0.3 (0.1) |
| SRB2 | 13.8 (0.5) | 7.6 (1.1) | 13.2 (2.7) | 68.8 (21.5) | 1.3 (0.3) | 1.4 (0.5) | 11.2 (2.6) | 0.2 (0.1) | 0.14 (0.1) | 1.4 (0.4) |
| SRB3 | 15.6 (0.2) | 6.6 (0.2) | 7.8 (1.4) | 34.5 (9.5) | 5.4 (2.0) | 1.1 (0.1) | 13.4 (2.8) | 0.3 (0.1) | 0.05 (0.0) | 5.2 (0.6) |
| SRB4 | 15.0 (0.3) | 7.9 (0.5) | 10.4 (1.6) | 20.0 (0.5) | 5.0 (1.9) | 0.8 (0.1) | 5.7 (2.6) | 0.8 (0.4) | 0.44 (0.4) | 2.4 (1.0) |
| SRB5 | 18.7 (1.8) | 7.1 (0.9) | 3.7 (0.1) | 9.4 (2.7) | 0.7 (0.1) | 0.5 (0.2) | 2.9 (1.3) | 0.1 (0.0) | 0.32 (0.2) | 0.8 (0.0) |





BGD
12, 12121–12156, 2015



**Table 2.** Phytoplankton planktonic pigments as ratios to chlorophyll *a* ($\mu g\,\mu g^{-1}$) in subarctic water bodies sampled in 2012.

| Sites | Photosynthetic | | | | Photoprotective | | | | | |
|---|---|---|---|---|---|---|---|---|---|---|
| | Allo | Chl *b* | Fuco | Perid | Cantha | Diadino | Echin | Lut | Viola | Zea |
| Thaw lakes on marine clays | | | | | | | | | | |
| BGR1 | 0.195 | 0.120 | 0.140 | 0.026 | 0.000 | 0.081 | 0.031 | 0.088 | 0.097 | 0.056 |
| BGR2 | 0.015 | 0.072 | 0.202 | 0.109 | 0.021 | 0.141 | 0.024 | 0.106 | 0.133 | 0.193 |
| NASA | 0.287 | 0.089 | 0.016 | 0.000 | 0.000 | 0.000 | 0.000 | 0.104 | 0.045 | 0.000 |
| NASH | 0.052 | 0.107 | 0.280 | 0.000 | 0.060 | 0.155 | 0.066 | 0.068 | 0.196 | 0.553 |
| Thaw lakes on mineral clays | | | | | | | | | | |
| KWK1 | 0.040 | 0.167 | 0.051 | 0.032 | 0.009 | 0.245 | 0.012 | 0.090 | 0.056 | 0.023 |
| KWK6 | 0.051 | 0.251 | 0.103 | 0.017 | 0.019 | 0.084 | 0.000 | 0.276 | 0.169 | 0.116 |
| KWK12 | 0.067 | 0.075 | 0.154 | 0.039 | 0.011 | 0.086 | 0.020 | 0.079 | 0.087 | 0.026 |
| KWK23 | 0.099 | 0.133 | 0.204 | 0.023 | 0.016 | 0.160 | 0.009 | 0.228 | 0.168 | 0.243 |
| Thaw lakes on peatlands | | | | | | | | | | |
| SAS1A | 0.118 | 0.049 | 0.299 | 0.029 | 0.020 | 0.071 | 0.000 | 0.038 | 0.092 | 0.022 |
| SAS1B | 0.145 | 0.059 | 0.236 | 0.055 | 0.006 | 0.061 | 0.000 | 0.040 | 0.061 | 0.011 |
| SAS2A | 0.166 | 0.042 | 0.112 | 0.000 | 0.000 | 0.023 | 0.000 | 0.023 | 0.000 | 0.000 |
| SAS2B | 0.370 | 0.160 | 0.357 | 0.000 | 0.022 | 0.031 | 0.027 | 0.135 | 0.111 | 0.000 |
| Shallow rock-basin lakes | | | | | | | | | | |
| SRB1 | 0.049 | 0.167 | 0.160 | 0.051 | 0.000 | 0.073 | 0.022 | 0.124 | 0.199 | 0.071 |
| SRB2 | 0.109 | 0.196 | 0.233 | 0.025 | 0.020 | 0.045 | 0.031 | 0.128 | 0.108 | 0.034 |
| SRB3 | 0.127 | 0.070 | 0.291 | 0.036 | 0.013 | 0.059 | 0.027 | 0.069 | 0.122 | 0.066 |
| SRB4 | 0.037 | 0.129 | 0.258 | 0.022 | 0.006 | 0.065 | 0.031 | 0.133 | 0.143 | 0.040 |
| SRB5 | 0.047 | 0.055 | 0.349 | 0.003 | 0.007 | 0.063 | 0.022 | 0.046 | 0.151 | 0.062 |

Key: Allo, alloxanthin; Chl *b*, chlorophyll *b*; Fuco, fucoxathin; Perid, peridinin; Cantha, canthaxanthin; Diadino, diadinoxanthin; Echin, echinenone; Lut, lutein; Viola, violaxanthin; Zea, zeaxanthin.





BGD
12, 12121–12156, 2015



**Table 3.** The relative concentration of bacteriochlorophyll *d* (BChl *d*, $\mu g L^{-1}$) based on the maximum peak area at 430 nm. The lakes have been arranged from lowest to highest concentrations.

| Site | Date | Depth (m) | BChl *d* ($\mu g L^{-1}$) |
|---|---|---|---|
| KWK6 | 4 Aug 2012 | 3.1 | 1.2 |
| KWK6 | 21 Aug 2011 | 3.1 | 1.3 |
| KWK23 | 4 Aug 2012 | 2.0 | 1.9 |
| KWK12 | 3 Aug 2012 | 2.0 | 8.2 |
| KWK12 | 19 Aug 2011 | 2.5 | 24.6 |
| KWK1 | 19 Aug 2011 | 2.0 | 28.9 |
| KWK23 | 4 Aug 2012 | 3.3 | 36.2 |
| KWK23 | 21 Aug 2011 | 3.3 | 44.3 |
| KWK1 | 3 Aug 2012 | 2.0 | 44.7 |
| KWK12 | 3 Aug 2012 | 2.5 | 47.3 |





BGD
12, 12121–12156, 2015



**Table 4.** RNA sequence analysis of eukaryotes in samples from permafrost thaw lake SAS2A, sampled in 2012. Each value is the % number of reads of the total for each sample (total number of reads minus rotifer sequences). The large fraction was retained on a 3 µm filter and the small fraction was on a 0.2 µm filter after filtration through the 3 µm pre-filter.

| Taxonomic group | Percentage of reads | | | |
|---|---|---|---|---|
| | Surface | | Bottom | |
| | Large | Small | Large | Small |
| Ciliophora | 22.94 | 43.55 | 62.95 | 83.90 |
| Dinophyta | 17.11 | 4.02 | 8.71 | 1.90 |
| Chrysophyta[a] | 14.47 | 14.81 | 9.07 | 3.60 |
| Chlorophyta[b] | 9.97 | 2.03 | 2.11 | 0.40 |
| Cercozoa | 6.17 | 12.37 | 2.50 | 1.22 |
| Cryptophyta | 3.10 | 1.71 | 2.39 | 0.65 |
| Katablepharidophyta | 2.71 | 1.00 | 0.11 | 0.20 |
| Bacillariophyta | 2.47 | 0.44 | 0.96 | 0.45 |
| Fungi[c] | 1.47 | 0.61 | 0.32 | 0.04 |
| Centroheliozoa | 1.44 | 0.80 | 0.11 | 0.12 |
| Choanoflagellida | 1.32 | 3.12 | 0.23 | 0.20 |
| Raphidophyceae | 0.51 | 0.33 | 0.00 | 0.04 |
| Pavlovales | 0.44 | 0.19 | 0.18 | 0.04 |
| Prymnesiales | 0.15 | 0.03 | 0.06 | 0.00 |
| Perkinsea | 0.00 | 0.00 | 0.03 | 0.12 |
| Unknown affinities | 15.75 | 15.00 | 10.28 | 7.11 |

[a] Includes Chrysophyceae, Synurophyceae and Bicosoecida.
[b] Includes Chlorophyceae and Trebouxiophyceae.
[c] Includes Chytridiomycota, Oomycota and Ascomycota.





BGD
12, 12121–12156, 2015



**Table 5.** Closest identity (ID) of eukaryotic RNA sequences from permafrost thaw lake SAS2A to GenBank sequences (following a BLASTn search), at the lowest taxonomic level identified.

| GenBank Taxonomy | Accession number | Isolation source | % ID | Percentage of reads | |
|---|---|---|---|---|---|
| | | | | Surface | Bottom |
| Ciliophora | | | | | |
| *Stokesia vernalis* | HM030738 | Freshwater | 99 | 8.65 | 0.04 |
| *Cryptocaryon* sp. | JF317699 | Drinking water | 99 | 0.89 | 5.61 |
| *Peniculida* sp. | GQ330632 | Peat bog water | 98 | 0.83 | 1.85 |
| *Halteria* sp. | GU067995 | Lake Esch-sur-Sure | 99 | 0.49 | 6.38 |
| *Cyclidium marinum* | JQ956553 | Marine coast | 99 | 0.00 | 34.42 |
| Chrysophyta | | | | | |
| *Uroglena* sp. | EU024983 | FU44-26 | 99 | 6.03 | 0.03 |
| *Paraphysomonas* sp. | JQ967316 | Freshwater | 99 | 0.67 | 3.78 |
| *Dinobryon divergens* | KJ579346 | WO33_4 | 99 | 0.40 | 0.00 |
| *Spumella-like flagellate* | AY651098 | Lake Mondsee | 99 | 0.03 | 0.76 |
| Rhizaria | | | | | |
| *Cercozoa* | AB771834 | Lake Kusaki | 99 | 3.83 | 0.28 |
| Cryptophyta | | | | | |
| *Cryptomonas tetrapyrenoidosa* | KF907407 | Deokam032610 | 99 | 1.71 | 0.87 |
| *Cryptomonas pyrenoidifera* | KF907397 | CNUCRY 166 | 99 | 0.33 | 0.00 |
| *Cryptomonas curvata* | KF907377 | CNUCRY 90 | 99 | 0.06 | 0.28 |
| Dinophyta | | | | | |
| *Dinophyceae* sp. | GQ423577 | Lake Baikal | 99 | 1.31 | 0.58 |
| *Peridinium wierzejskii* | KF446619 | Baikal region | 99 | 1.03 | 2.07 |
| *Gyrodiniellum shiwhaense* | FR720082 | Shiwha Bay | 98 | 0.49 | 0.01 |
| Bacillariophyta | | | | | |
| *Urosolenia eriensis* | HQ912577 | Y98-8 | 98 | 1.22 | 0.58 |
| *Urosolenia eriensis* | HQ912577 | Y98-8 | 99 | 0.22 | 0.10 |
| Chlorophyta | | | | | |
| *Lemmermannia punctata* | JQ356704 | SAG 25.81 | 99 | 1.07 | 0.08 |
| *Chlorella* sp. | Y12816 | OvS/Ger1 | 99 | 1.00 | 0.00 |
| *Choricystis* sp. | AY195972 | AS-29 | 99 | 0.89 | 0.11 |
| *Koliella longiseta* | HE610126 | SAG 470-1 | 99 | 0.72 | 0.04 |
| *Monoraphidium* sp. | KP017571 | LB59 | 99 | 0.39 | 0.00 |
| Raphidophyta | | | | | |
| *Gonyostomum semen* | KP200894 | Freshwater | 100 | 0.23 | 0.02 |
| Fungi | | | | | |
| *Saprolegnia* sp. | FJ794911 | Lake (parasite) | 99 | 0.11 | 0.00 |
| *Penicillium brevicompactum* | KP981369 | ATCC 16024 | 99 | 0.00 | 0.10 |
| Prymnesiales | | | | | |
| *Chrysochromulina parva* | EU024987 | FU44-40 | 100 | 0.09 | 0.03 |





BGD
12, 12121–12156, 2015




**Figure 1.** The location of the study area in subarctic Quebec.





BGD
12, 12121–12156, 2015



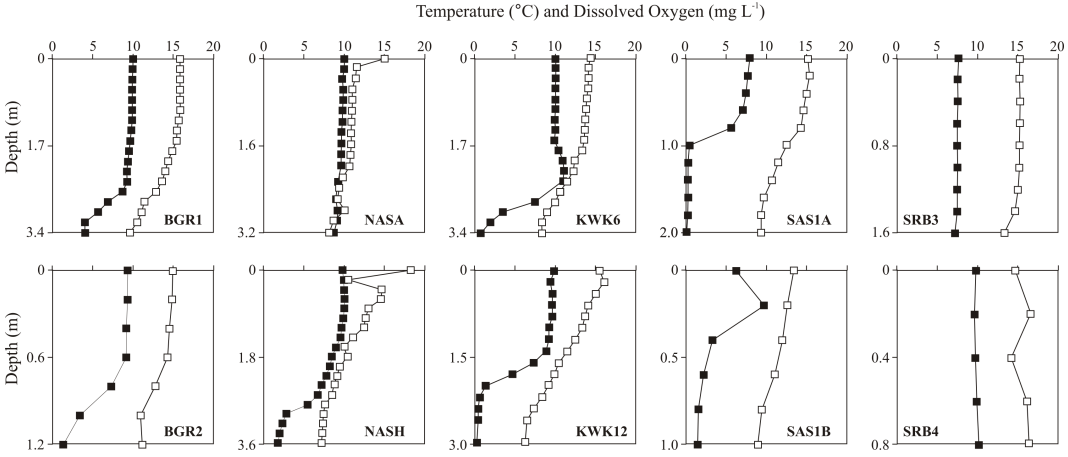


**Figure 2.** Temperature (white squares) and oxygen (black squares) profiles in permafrost thaw lakes (BGR, KWK, NAS, SAS) and shallow rock-basin lakes (SRB) during the summer 2012.





BGD
12, 12121–12156, 2015



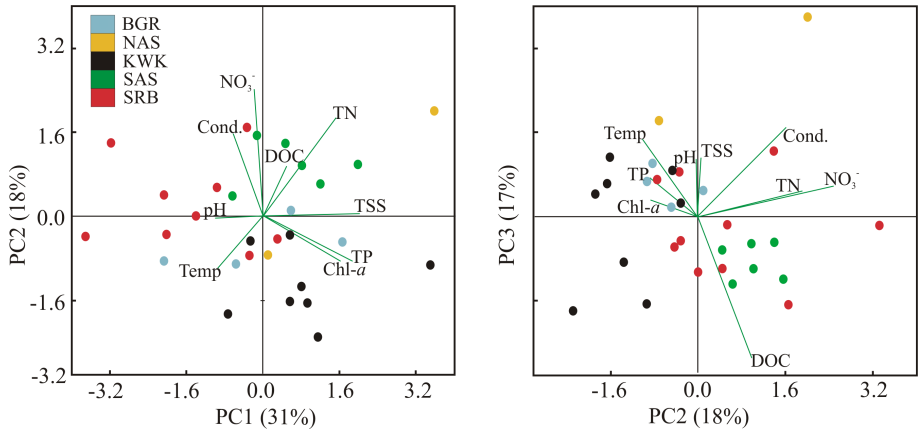


**Figure 3.** Principal component analysis of limnological variables in the thaw and SRB lakes. The first and second factors (left hand panel) account for 49 % of the variability and the second and third factors (right hand panel) account for 35 % of the variability.





BGD
12, 12121–12156, 2015



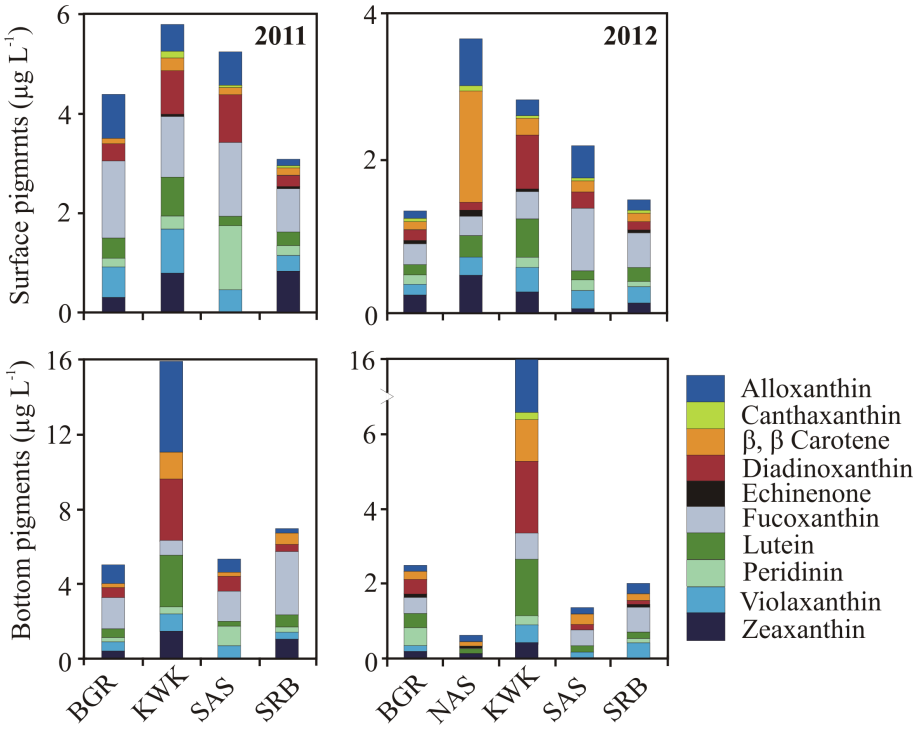


**Figure 4.** Average phytoplankton pigment compositions in the permafrost thaw and SRB lakes in surface and bottom waters.





BGD
12, 12121–12156, 2015



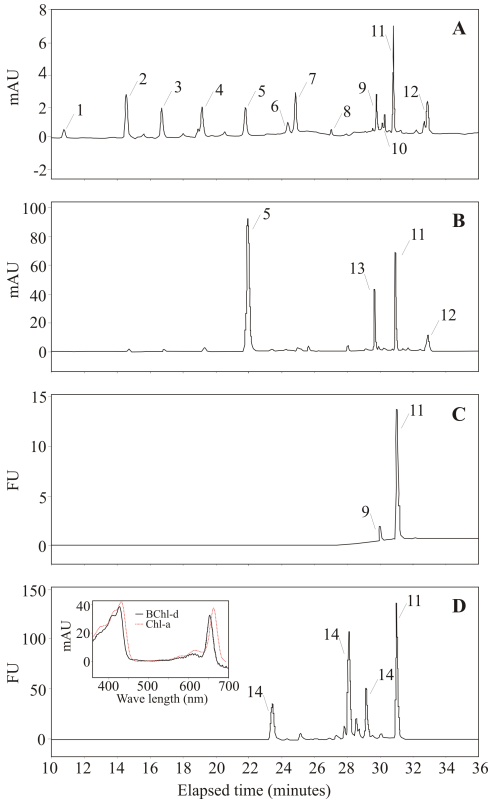


**Figure 5.** High-performance liquid chromatograms of the KWK12 lake: absorbance for the surface **(a)** or bottom **(b)** water layers and fluorescence for the surface **(c)** or bottom **(d)** water layers. Pigments from left to right: 1. Perid, 2. Fuco, 3. Viola, 4. Diadino, 5. Allo, 6. Zea, 7. Lut, 8. Cantha, 9. Chl *b*, 10. Echin, 11. Chl *a*, 12. $\beta$,$\beta$-Carotene, 13. Croco and 14. BChl *d*. Insert in **(d)**: Bacteriochlorophyll Chl *d* (BCHl *d*, black line) and Chl *a* (red line) absorption spectra (mAU = measured absorption units).





BGD
12, 12121–12156, 2015



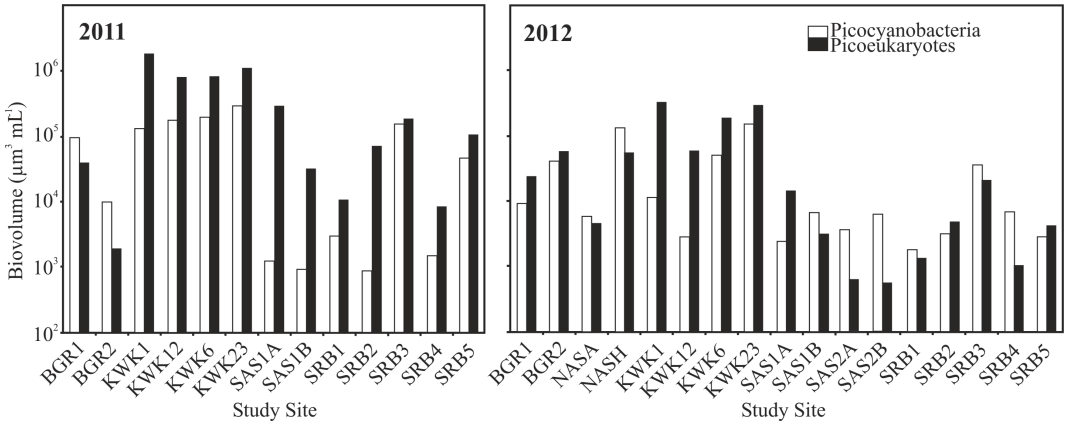


**Figure 6.** Picophytoplankton biovolume in the surface water of shallow rock-basin (SRB) and permafrost thaw lakes located on marine clays (KWK, BGR, NAS) and peatlands (SAS).





BGD
12, 12121–12156, 2015